



HAL
open science

Wide range local resistance imaging on fragile materials by conducting probe atomic force microscopy in intermittent contact mode

Aymeric Vecchiola, Pascal Chrétien, Sophie Delprat, Karim Bouzehouane,
Olivier Schneegans, Pierre Seneor, Richard Mattana, Sergio Tatay, Bernard
Geffroy, Yvan Bonnassieux, et al.

► To cite this version:

Aymeric Vecchiola, Pascal Chrétien, Sophie Delprat, Karim Bouzehouane, Olivier Schneegans, et al..
Wide range local resistance imaging on fragile materials by conducting probe atomic force microscopy
in intermittent contact mode. *Applied Physics Letters*, 2016, 108, pp.243101. 10.1063/1.4953870 .
cea-01331971

HAL Id: cea-01331971

<https://cea.hal.science/cea-01331971>

Submitted on 15 Jun 2016

HAL is a multi-disciplinary open access archive for the deposit and dissemination of scientific research documents, whether they are published or not. The documents may come from teaching and research institutions in France or abroad, or from public or private research centers.

L'archive ouverte pluridisciplinaire **HAL**, est destinée au dépôt et à la diffusion de documents scientifiques de niveau recherche, publiés ou non, émanant des établissements d'enseignement et de recherche français ou étrangers, des laboratoires publics ou privés.

Wide range local resistance imaging on fragile materials by conducting probe atomic force microscopy in intermittent contact mode

Aymeric Vecchiola, Pascal Chrétien, Sophie Delprat, Karim Bouzehouane, Olivier Schneegans, Pierre Seneor, Richard Mattana, Sergio Tatay, Bernard Geffroy, Yvan Bonnassieux, Denis Mencaraglia, and Frédéric Houzé

Citation: *Applied Physics Letters* **108**, 243101 (2016); doi: 10.1063/1.4953870

View online: <http://dx.doi.org/10.1063/1.4953870>

View Table of Contents: <http://scitation.aip.org/content/aip/journal/apl/108/24?ver=pdfcov>

Published by the [AIP Publishing](#)

Articles you may be interested in

Potential dependent change in local structure of ferrocenyl-terminated molecular islands by electrochemical frequency modulation atomic force microscopy

J. Vac. Sci. Technol. B **28**, C4D40 (2010); 10.1116/1.3316501

Electrical transport and mechanical properties of alkylsilane self-assembled monolayers on silicon surfaces probed by atomic force microscopy

J. Chem. Phys. **130**, 114705 (2009); 10.1063/1.3089789

Orientation-dependent conductance study of pentacene nanocrystals by conductive atomic force microscopy

Appl. Phys. Lett. **93**, 053304 (2008); 10.1063/1.2960343

Simultaneous resistance and capacitance cartography by conducting probe atomic force microscopy in contact mode

Appl. Phys. Lett. **86**, 123103 (2005); 10.1063/1.1886262

Electrical measurements of a dithiolated electronic molecule via conducting atomic force microscopy

Appl. Phys. Lett. **81**, 3043 (2002); 10.1063/1.1512815

The advertisement for MMR Technologies features a blue and white background with a grid pattern. On the left is the MMR Technologies logo, which consists of a stylized 'M' and 'R' in a blue and red arc, with 'TECHNOLOGIES' written below. To the right of the logo is the text 'THE WORLD'S RESOURCE FOR VARIABLE TEMPERATURE SOLID STATE CHARACTERIZATION' in bold, black, uppercase letters. Below this text are five images of different scientific instruments: 1. Optical Studies Systems, showing a small white device and a blue probe. 2. Seebeck Studies Systems, showing a blue device labeled 'SB1000' and 'K2000'. 3. Microprobe Stations, showing a white circular device with multiple ports. 4. Hall Effect Study Systems and Magnets, showing a blue device labeled 'MS000' and 'K2000' next to a small metal component. 5. A large, complex mechanical device with multiple rollers and a central shaft.

WWW.MMR-TECH.COM

OPTICAL STUDIES SYSTEMS SEEBECK STUDIES SYSTEMS MICROPROBE STATIONS HALL EFFECT STUDY SYSTEMS AND MAGNETS

Wide range local resistance imaging on fragile materials by conducting probe atomic force microscopy in intermittent contact mode

Aymeric Vecchiola,^{1,2,3} Pascal Chrétien,¹ Sophie Delprat,^{3,4} Karim Bouzehouane,³ Olivier Schneegans,¹ Pierre Seneor,³ Richard Mattana,³ Sergio Tatay,⁵ Bernard Geffroy,^{6,7} Yvan Bonnassieux,⁶ Denis Mencaraglia,¹ and Frédéric Houzé^{1,a)}

¹Laboratoire de Génie électrique et électronique de Paris (GeePs), UMR 8507 CNRS-CentraleSupélec, Paris-Sud and UPMC Universities, 11 rue Joliot-Curie, Plateau de Moulon, 91192 Gif-sur-Yvette, France

²Concept Scientific Instruments, ZA de Courtaboeuf, 2 rue de la Terre de Feu, 91940 Les Ulis, France

³Unité Mixte de Physique CNRS-Thales UMR 137, 1 avenue Augustin Fresnel, 91767 Palaiseau, France

⁴UPMC, Université Paris 06, 4 place Jussieu, 75005 Paris, France

⁵Molecular Science Institute, University of Valencia, 46980 Paterna, Spain

⁶Lab. Physique des Interfaces et Couches minces (PICM), UMR 7647 CNRS-École polytechnique, 91128 Palaiseau, France

⁷Lab. d'Innovation en Chimie des Surfaces et Nanosciences (LICSEN), NIMBE UMR 3685 CNRS-CEA Saclay, 91191 Gif-sur-Yvette, France

(Received 17 December 2015; accepted 25 May 2016; published online 14 June 2016)

An imaging technique associating a slowly intermittent contact mode of atomic force microscopy (AFM) with a home-made multi-purpose resistance sensing device is presented. It aims at extending the widespread resistance measurements classically operated in contact mode AFM to broaden their application fields to soft materials (molecular electronics, biology) and fragile or weakly anchored nano-objects, for which nanoscale electrical characterization is highly demanded and often proves to be a challenging task in contact mode. Compared with the state of the art concerning less aggressive solutions for AFM electrical imaging, our technique brings a significantly wider range of resistance measurement (over 10 decades) without any manual switching, which is a major advantage for the characterization of materials with large on-sample resistance variations. After describing the basics of the set-up, we report on preliminary investigations focused on academic samples of self-assembled monolayers with various thicknesses as a demonstrator of the imaging capabilities of our instrument, from qualitative and semi-quantitative viewpoints. Then two application examples are presented, regarding an organic photovoltaic thin film and an array of individual vertical carbon nanotubes. Both attest the relevance of the technique for the control and optimization of technological processes. *Published by AIP Publishing.*

[<http://dx.doi.org/10.1063/1.4953870>]

For the last two decades, conducting probe Atomic Force Microscope (cp-AFM) has proved to be a versatile and powerful tool for the simultaneous measurement of topography and various electrical properties (resistance, capacitance, potential, etc.) at nanometer scale on a wide variety of materials and devices. Regarding local resistance—or conductivity—measurements, various techniques based on different sensors and amplifiers have been proposed, depending on the current range aimed at.^{1–6} However in all these historical current-sensing techniques, AFM was operated in its standard contact mode, namely, in the repulsive-force regime, which is not well-suited for studying delicate samples such as ultrathin organic layers or fragile or poorly anchored nano-objects, very sensitive to the lateral shear forces resulting from the scanning motion. These forces not only can damage such samples but also the particles or debris produced can stick to the tip apex thus impairing measurement quality. The noncontact mode is a radical mean to prevent such degradations by the complete suppression of their cause, but to the detriment of the resolution and preventing any conductivity measurement. Alternatively, a solution

based on the excitation of a torsional resonance of the cantilever has been proposed to achieve lower force scanning while maintaining the tip in the near-field but has remained less used, although compatible with electrical mapping.⁷ Finally, the introduction of intermittent contact modes brought a neat compromise solution for a significant reduction of lateral forces, allowing non-destructive multipurpose imaging on delicate samples.

The common principle of these modes consists of oscillating the probe or the sample in close proximity to each other so that the tip furtively hits the sample surface at each period of oscillation. In the most utilized intermittent technique, referred to as “tapping-mode,”⁸ a quite stiff AFM cantilever is oscillated near its flexural resonance frequency (typically in the range of 100–300 kHz) and the feedback parameter is usually the amplitude reduction of cantilever vibration. This operating mode offers a high spatial resolution by allowing the use of sharper tips than in the contact mode, but has the disadvantage that the normal force acting on the sample surface is difficult to quantify. Furthermore, the extremely short contact duration (typically less than 1 μ s) is a serious impediment to proper conductivity measurements with acceptable signal-to-noise ratio.⁹ That is why techniques involving much lower operating frequencies

^{a)}Author to whom correspondence should be addressed. Electronic mail: frederic.houze@gpeps.centralesupelec.fr

(typically 10^2 to a few 10^3 Hz) have been preferred for simultaneous topography and conductivity measurement in an intermittent mode,^{10,11} some being currently commercially available.¹¹ These techniques were all inspired by the so-called pulsed force mode (PFM) non-resonant actuation concept, originally developed for local mechanical investigation.^{12,13} From the electrical viewpoint, the main commercially available systems^{14–16} are associated with linear amplification based devices; as a result, their measurement range is restricted to 3–4 orders of magnitude—possibly shifted by manual switching. As a break with this state of the art, we propose in this paper to associate the PFM actuation with a specifically adapted version of our conversion and amplification (not logarithmic but of log-type) module named “Resiscope,”⁶ providing as a result direct resistance measurements over 10 orders of magnitude without any operator intervention. In addition, we bring the possibility to precisely define for each intermittency cycle the moment at which the electrical information is collected, which is of crucial importance concerning a log-like signal (see below).

The basic principle of the PFM mode consists of introducing a sinusoidal modulation on the AFM *z*-piezo at a frequency between 100 Hz and 2 kHz (far below cantilever fundamental resonance), with the amplitude adjusted so that the tip jumps in and off contact every cycle. The maximum repulsive force is measured from the deflection signal and used as a feedback parameter, ensuring well-controlled scan conditions for delicate samples. In the standard use of PFM, the succession of so obtained force-distance curves is analyzed to produce images of local stiffness and adhesion simultaneously with topography. Besides these mechanical data—not considered further in the paper—specific investigations regarding electrical properties can be achieved by using conducting probes. When a DC bias voltage is applied between tip and sample, a current may flow during the brief contact time of each cycle (typical duration of tens or hundreds of μ s), depending on the local conductivity. The measurement of this intermittent current is a challenging task compared with the case of permanent contact mode initially addressed by our amplification and conversion Resiscope device,⁶ which practically brought us to upgrade it with some adaptations. In particular, its electronic circuit was redesigned to minimize parasitic capacitances and thus reduce time constant. Moreover, the careful observation of deflection and current signals with an oscilloscope revealed that the tip/sample resistance generally reaches its minimum value after maximum force has occurred, with a time shift (Δt) much longer than the Resiscope response time itself (which is about 20 μ s). This time shift was found to depend on the sample nature (measurements were made on evaporated Au, cleaved HOPG, and doped Si as reference samples) and to decrease when the actuation frequency or amplitude is decreased. At the moment, its origin is not clearly identified and is still under investigation. As a pragmatic mean to overcome this impediment, we synchronized signal acquisition the closest to the minimum resistance, rather than with the force peak as could have been done intuitively. It is worth noting that an integration over all or part of the force cycle duration, as is common practice with linear amps, would be nonsense for our log-like signal. As a result of these

optimizations, the modified Resiscope enables to cover 10 decades from 10^2 to 10^{12} Ω (or 10^3 to 10^{13} Ω in a variant ranging version) for PFM operating frequencies up to 2 kHz. The rest of the measurement platform, i.e., the microscopy core was composed of commercial equipments, namely, an Agilent Technologies 5500 AFM system to which a fully adjustable analog PFM apparatus from Witec was added as external module. A schematic view of the experimental set-up is presented in Figure 1(a). Figures 1(b) and 1(c) show examples of time evolution of measured signals and of resistance map, respectively, for a reference HOPG sample.

On such a sample, the resistance values are found less than an order of magnitude higher in PFM than in contact mode for low setpoint forces (nN range) and same tip. This

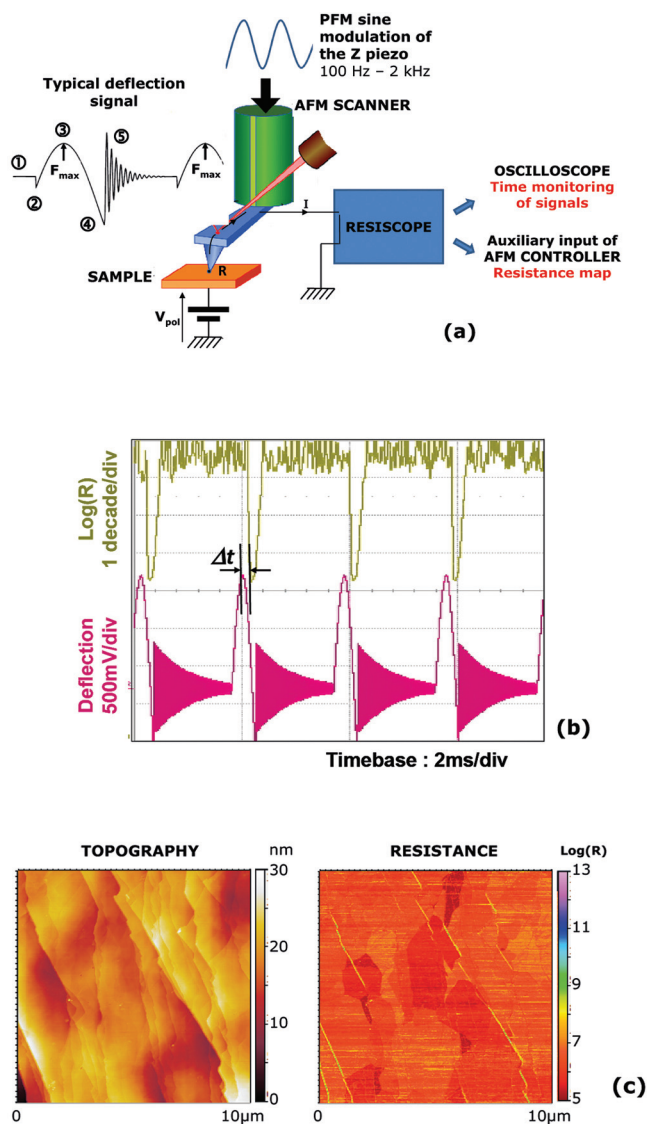


FIG. 1. (a) Schematic view of the PFM-AFM-Resiscope set-up we used for local resistance measurements in intermittent contact mode. The small graph on the left side shows the successive phases of a deflection versus time curve, i.e., tip approach without interaction ①, jump-to-contact ②, maximum of repulsive force ③, adhesion peak at withdrawal ④, and jump-off and free cantilever oscillation ⑤. (b) Example of oscilloscope capture illustrating a variation of more than 2 decades between $\text{Log}(R)$ at the maximum deflection and the minimum value of $\text{Log}(R)$; the corresponding time shift Δt is about 160 μ s, that is to say, more than 8 times the Resiscope response time (HOPG sample, PtIr coated tip, $f = 512$ Hz, $F_{\text{max}} = 300$ nN). (c) Example of topography and resistance images (HOPG sample, Cr/Pt coated tip, $f = 540$ Hz, $F_{\text{max}} = 150$ nN).

differential declines when setpoint force is increased (tens or hundreds of nN). We think that the lowering of resistance values in contact mode compared with PFM is simply due to friction which increases the tip-sample contact area.

In order to prove the ability of our instrumentation to get some qualitative and even semi-quantitative electrical information on fragile samples, self-assembled monolayers (SAMs) of alkanethiols with various chain lengths deposited on the gold-coated substrates were chosen as demonstration objects. SAMs are indeed a quite simple mean to get ideal reference large-sized surfaces with high molecular organisation and well-defined thickness. SAMs of unsaturated or saturated thiols have been extensively considered as model systems to investigate electron transport mechanisms through ultrathin molecular films by various methods.^{17–23} For such a situation of a molecular layer with a wide gap between its highest occupied molecular orbital (HOMO) and lowest unoccupied molecular orbital (LUMO), as is the case of alkanethiols, sandwiched between two metal contacts, the conduction mechanism is expected to be direct tunnelling,²³ with resistance increasing exponentially with molecular length l following the law $R \propto \exp(\beta l)$, the so-called attenuation factor β being larger for saturated alkanethiols than for conjugated ones.

Practically our SAMs were formed by $\text{CH}_3-(\text{CH}_2)_n-\text{SH}$ molecules with $n = 5, 7, 9, 11, \text{ or } 13$, hereafter referred to as the number of carbon atoms in their chains, i.e., as C6, C8, C10, C12, C14 samples, respectively. Monolayers were formed immersing gold substrates cleaned using piranha solution into 1 mM ethanol solutions containing alkylthiols of different chain lengths. After 16 h the samples were rinsed with ethanol and blown dry under nitrogen. The quality of the SAM monolayers was checked by contact angle measurements and AFM. Samples had contact angles between 102° and 109° for all chain lengths (C6–C14).

To avoid contamination or possible degradation at room atmosphere, SAM samples were stored in a nitrogen box up to PFM-Resiscope measurements. The best-suited experimental conditions for these layers were: use of probes with Cr/Pt conductive coating and low stiffness cantilevers (0.2 N/m), maximum normal force of 25 nN, operating PFM frequency of 1600 Hz and sample to tip polarization of 1 V. From 3 to 5 rectangular scans of $1 \mu\text{m} \times 0.5 \mu\text{m}$ were performed on each surface. All the topography maps revealed the small grain structure of the substrate (30 nm sputtered gold on silicon), as illustrated by the height image of a C10 sample presented in Figure 2. A Gaussian law can satisfactorily fit the distribution of heights derived from these maps with a FWHM (full width at half maximum) ranging between 0.4 nm and 0.7 nm. This value is comparable to that obtained for 30 nm bare gold reference samples.

Figure 3 shows using the same color scale typical resistance maps obtained for the 5 chain lengths studied. For each image, tens of thousands measurement points are involved (512×256), so that the mean value of $\text{Log}(R)$ is a statistical meaningful electrical characterization parameter. Figure 4 represents the calculated mean $\text{Log}(R)$ values as a function of the SAM chain length; the error bars correspond to the associated standard deviations; for each chain length, data correspond to different zones of the same sample and have been slightly shifted for clarity. One can observe that the

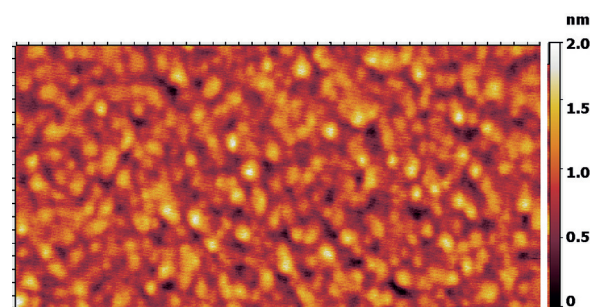


FIG. 2. Typical topography map ($1 \mu\text{m} \times 0.5 \mu\text{m}$) obtained by PFM-Resiscope with a Cr/Pt-coated tip on a C10 sample, showing the small grains of the gold substrate. In this case, the FWHM parameter of the Gaussian distribution of heights is 0.54 nm.

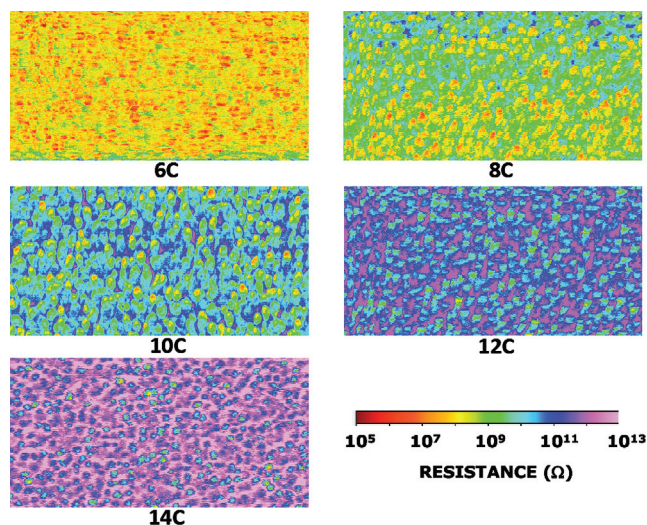


FIG. 3. Typical resistance maps ($1 \mu\text{m} \times 0.5 \mu\text{m}$) obtained by PFM-Resiscope with a Cr/Pt-coated tip on the series of alkanethiol SAMs with 5 different chain lengths.

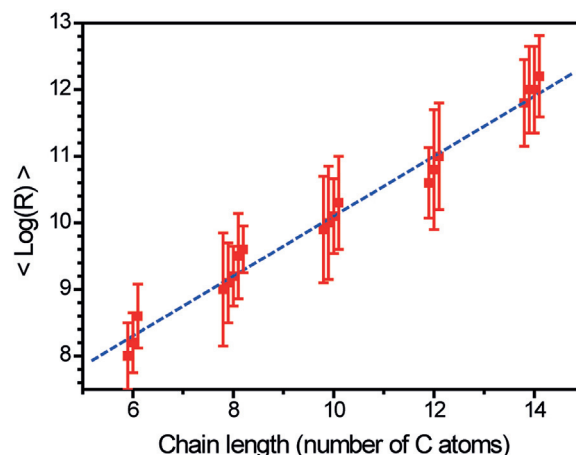


FIG. 4. Summing-up of mean $\text{Log}(R)$ values (square symbols, slightly shifted along each C number for clarity, 1 sample per C number, from 3 to 5 zones per sample) and associated standard deviation (error bars) calculated from the resistance maps obtained by PFM-Resiscope on the SAMs layers, and linear fit of the data (dotted line). The deduced attenuation factor is $\beta = 1.04/\text{C atom}$ (0.83 \AA^{-1}), in agreement with the values reported in the literature.

mean values data are quite well linearly fitted, with a typical attenuation factor β of 1.04 per C atom, that is to say, 0.83 \AA^{-1} , which is in accordance with the results reported in the literature using a cp-AFM with a metal-coated tip to form metal-molecule-metal junctions in a configuration similar to ours.^{17,18} The large dispersion of $\text{Log}(R)$ values (from 0.7 to 1.8) can be attributed to the height variations associated with the gold grains structure depicted above. In fact, by considering the cartographies of “error signal” (i.e., the difference between theoretical setpoint deflection and actual measured deflection) associated with each image, we inferred that slight variations of the actual maximum force may occur for the highest grains. Such brief and tiny deviations of maximum force are significant enough to induce small variations in the SAM layers squeezing, with exponential repercussion on the tunnelling current. Typical SAMs defects such as molecular packing or tilt angle variation can also contribute to resistance dispersion.

Beyond academic samples like SAMs, Resiscope in intermittent mode may open up interesting prospect for concrete technological applications, such as organic solar cells which are extensively studied in the race to low-cost solutions for solar energy harvesting. As a meaningful example, we propose to have an insight into imaging one of the most common active layers involved in these devices. It consists of a blend of poly (3-hexylthiophene) (P3HT), a conjugated polymer acting as a donor, and [6,6]-phenyl C61-butyric acid methyl ester (PCBM), a fullerene derivative acting as acceptor, both organized in two three-dimensional interpenetrating networks named bulk heterojunctions (BHJ). The size and relative spatial arrangement of donor and acceptor phases result from elaboration parameters and have a decisive influence on the final solar cell efficiency. In order to simplify the sample structure, the PEDOT:PSS (poly(3,4-ethylenedioxythiophene) polystyrene sulfonate) classically used in solar cells as a hole transport underlayer has been intentionally omitted. AFM appears as an ideal tool for the characterization of such BHJ blend at nanoscale. However, contact mode often proves to be poorly suited for polymer samples;²⁴ thus in the reference paper by Dante *et al.*, the authors combined tapping mode AFM for morphological imaging and contact conducting-AFM for charge transport study.²⁵ Far from a very extensive work, we only intend hereafter showing that the Resiscope in a pulsed force mode can bring a relevant answer in such a challenging situation.

Our P3HT:PCBM films (90 nm thick) were obtained by spin-coating of a 1,2-dichlorobenzene (DCB from Sigma Aldrich) solution of the two organic components onto an indium tin oxide (ITO)-covered glass substrate. Preliminary to electrical measurements, we established that a force setpoint of 50 nN can be used in PFM without causing any apparent damage to the samples, whereas a 5 nN force in contact mode proves to be enough to degrade surfaces. Figure 5 shows typical $2 \mu\text{m} \times 2 \mu\text{m}$ topography and resistance maps obtained with a PtIr-coated tip biased at -3 V (pulsed force modulation frequency 2 kHz, force setpoint 50 nN, scan rate 0.5 line/s). The topography image reveals granular features attributed to P3HT and/or PCBM aggregates. The electrical contrast of the resistance image, covering about 4 decades, has no clear correlation with height data and exhibits a

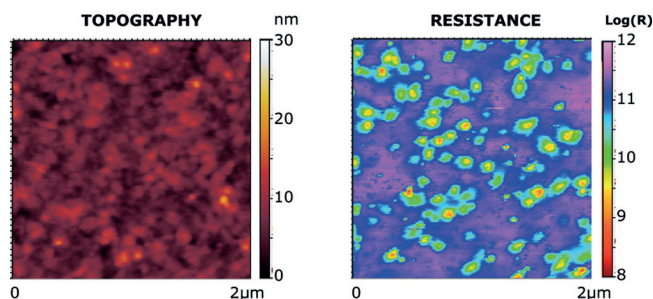


FIG. 5. Typical topography and resistance maps obtained by PFM-Resiscope with a PtIr-coated tip (-3 V biased) on a P3HT:PCBM solar cell active layer on ITO/glass substrate.

distribution of higher conductivity spots. Considering Figure 6, the energy levels of the HOMO and the LUMO of P3HT and PCBM, compared to PtIr and ITO work functions, one can verify that the HOMO of P3HT closely matches PtIr and ITO Fermi levels. Therefore, holes are the majority carriers and lower resistance areas (higher currents) come from hole transport along the P3HT, thus revealing P3HT domains vertically connected to the back ITO electrode. Conversely, higher resistance regions correspond either to PCBM domains or to non-connected materials. These qualitative results are comparable with those reported in Ref. 24 for a Pt-coated probe and provide valuable information for optimizing the active layer elaboration.

Finally, our third demonstrating example deals with imaging *extremely* brittle nano-objects: individual vertical carbon nanotubes (v-CNTs), 50–70 nm in diameter and about 500 nm in height, grown on a discoid TiN layer (Fig. 7, top left picture). Such v-CNTs were elaborated for field effect high-density electronic emission devices according to described procedures.²⁶ The resistance maps obtained on each v-CNT with typical maximum force between 5 and 10 nN (Fig. 7, top right picture), proved to be reproducible over several successive scans without any alteration (verified through height profiles), with resistance variations over 5–6 decades, which cannot be reached with a linear amp based device. Conversely, when operating in contact mode at the same forces, the nanotubes are systematically broken from the first scan. These results emphasize the relevance of the proposed technique for wide range of measurements on very sensitive devices.

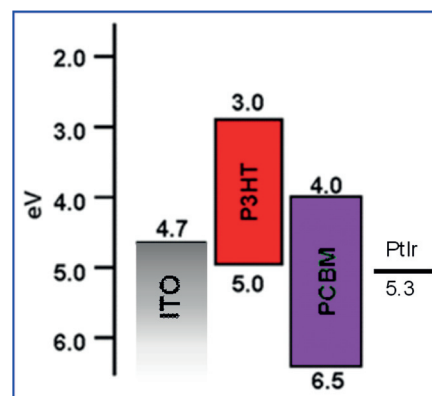


FIG. 6. Schematic diagram of energy levels (non contacting materials, referenced with respect to vacuum).

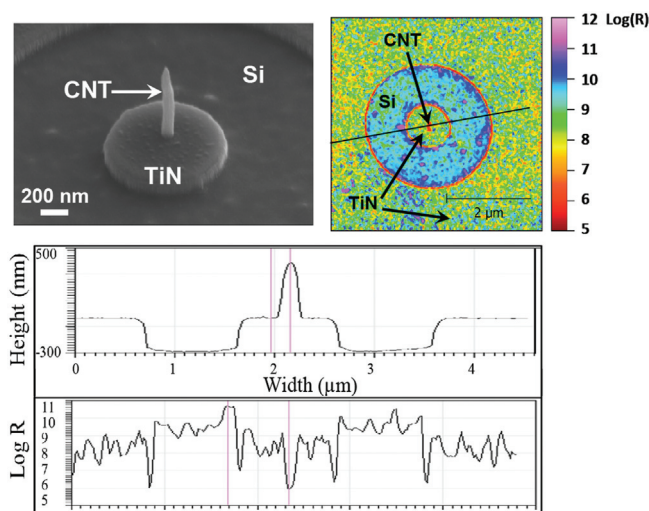


FIG. 7. Application of the PFM-Resiscope technique (max force 5–10 nN) for imaging individual vertical carbon nanotubes. The top left scanning electron microscopy image shows one of these nano-objects. The top right image corresponds to a typical resistance map, which proved to be reproducible over several successive scans (7 in the present case). The resistance profile (bottom curve) reveals variations over 5 decades. The height profile (upper line) allows to verify that the object is not altered by the scan. Conversely, when operating in contact mode at the same force, the nanotube is broken from the first scan.

In conclusion, we report in this paper on a cp-AFM technique associating “pulsed-force mode” intermittent AFM actuation with a home-made device allowing extremely wide-range (10 decades) local resistance measurements on sensitive samples. Study of self-assembled monolayers (SAMs) of alkanethiols with various chains verified that the measured resistance increases following the expected exponential variation with molecular length and evidenced the ability of our technique to get semi-quantitative results. On a more concrete application, our technique has proved to match up to state-of-art results obtained in contact mode on an organic absorber layer for solar cells (P3HT:PCBM blend), but in our case, with the considerable advantage of no degrading the sample surface as well as tip apex coating. Finally, using a much more original sample consisting in an array of vertical carbon nanotubes, we have demonstrated the usefulness of the large dynamic range of resistance offered by our set-up on extremely sensitive devices. Further work will be devoted to get a deeper understanding of the intermittent nanocontact physics (in particular, elucidating the origin of the offset between deflection and current signals) and its applicability to other fragile materials.

The authors gratefully acknowledge the French National Research Agency (ANR) for the financial support in the framework of its P2N Programme for Nanotechnologies and Nanosystems (“MELAMIN” project, ANR-2011-NANO-021). They also thank the National Association for Research and Technology (ANRT) and the scientific equipment manufacturer Concept Scientific Instruments (CSI) for funding A. Vecchiola’s

Ph.D. thesis. The P3HT:PCBM samples were elaborated by Appan Merari Masillamani, Post-Doc fellow funded in the framework of the project OPV Charge Transport supported by the French National Research Agency under the Program Investing in the Future Grant No. ANR-11-IDEX-0003-02 and launched by the department Triangle de la Physique (FCS, Fondation de coopération scientifique « Campus Paris Saclay ») and the LabEx CHARM₃AT and NanoSaclay. The vCNTs sample was elaborated by L. Gangloff from Thales Research and Technology Nanocarb team.

¹W. Vandervorst and M. Meuris, EP patent 466274 (1992); U.S. patent 5,369,372 (1994).

²F. Houzé, R. Meyer, O. Schneegans, and L. Boyer, *Appl. Phys. Lett.* **69**(13), 1975 (1996).

³O. Schneegans, Ph.D. thesis, Pierre et Marie Curie University, 1998.

⁴P. De Wolf, Ph.D. thesis, University of Leuven, 1998.

⁵L. Aguilera, M. Lanza, M. Porti, J. Grifoll, M. Nafria, and X. Aymerich, *Rev. Sci. Instrum.* **79**, 073701 (2008).

⁶O. Schneegans, P. Chrétien, and F. Houzé, WO patent application 2011138738A1 (2011); EP patent application 2567245A1 (2013).

⁷S. Weber, N. Haberkorn, P. Theato, and R. Berger, *Nano Lett.* **10**, 1194 (2010).

⁸Q. Zhong, D. Inniss, K. Kjoller, and V. B. Elings, *Surf. Sci.* **290**, L688 (1993).

⁹C. Noguez, S. R. Cohen, S. S. Daube, and R. Naaman, *Phys. Chem. Chem. Phys.* **6**, 4459 (2004).

¹⁰P. Eyben, M. Fouchier, P. Albart, J. Charon-Verstappen, and W. Vandervorst, *MRS Proceedings* **717**, C7.7.1 (2002).

¹¹C. Li, S. Minne, B. Pittenger, A. Mednick, M. Guide, and T.-Q. Nguyen, Bruker Application Note No. 132 (2011); S. Magonov, NTMDT Application Note No. 087 (2013).

¹²A. Rosa-Zeiser, E. Weilandt, S. Hild, and O. Marti, *Meas. Sci. Technol.* **8**, 1333 (1997).

¹³H.-U. Krottil, T. Stifter, H. Waschipyk, K. Weishaupt, S. Hild, and O. Marti, *Surf. Interface Anal.* **27**, 336 (1999).

¹⁴See http://www.lot-qd.de/files/downloads/witec/eu/conductivity_eu01.pdf for WITec focus innovations, 2008.

¹⁵See <http://usa.jpk.com/jpk-productnote-cafm-with-qi.download.c7ffdb011830d681791fbb6db5437b1b> for JPK product note.

¹⁶See https://www.bruker.com/fileadmin/user_upload/8-PDF-Docs/Surface Analysis/AFM/ApplicationNotes/Simultaneous_Electrical_and_Mechanical_Property_Mapping_at_the_Nanoscale_with_PeakForce_TUNA_AFM_AN132.pdf for Bruker application note #132.

¹⁷L. A. Bumm, J. J. Arnold, T. D. Dunbar, D. L. Allara, and P. S. Weiss, *J. Phys. Chem. B* **103**(38), 8122 (1999).

¹⁸D. J. Wold, R. Haag, M. A. Rampi, and C. D. Frisbie, *J. Phys. Chem. B* **106**(11), 2813 (2002).

¹⁹V. B. Engelkes, J. M. Beebe, and C. D. Frisbie, *J. Am. Chem. Soc.* **126**(43), 14287 (2004).

²⁰R. E. Holmlin, R. Haag, M. L. Chabynyc, R. F. Ismagilov, A. E. Cohen, A. Terfort, M. A. Rampi, and G. M. Whitesides, *J. Am. Chem. Soc.* **123**(21), 5075 (2001).

²¹J. G. Kushmerick, D. B. Holt, S. K. Pollack, M. A. Ratner, J. C. Yang, T. L. Schull, J. Naciri, M. H. Moore, and R. Shashidhar, *J. Am. Chem. Soc.* **124**(36), 10654 (2002).

²²J. F. Smalley, S. W. Feldberg, C. E. D. Chidsey, M. R. Linford, M. D. Newton, and Y. P. Lid, *J. Phys. Chem.* **99**(35), 13141 (1995).

²³W. Wang, T. Lee, and M. A. Reed, *Phys. Rev. B* **68**, 035416 (2003).

²⁴R. Giridharagopal, G. Shao, C. Groves, and D. S. Ginger, *Mater. Today* **13**(9), 50 (2010).

²⁵M. Dante, J. Peet, and T.-Q. Nguyen, *J. Phys. Chem. C* **112**, 7241 (2008).

²⁶L. Gangloff, E. Minoux, K. B. K. Teo, P. Vincent, V. T. Semet, V. T. Binh, M. H. Yang, I. Y. Y. Bu, R. G. Lacerda, G. Pirio, J. P. Schnell, D. Pribat, D. G. Hasko, G. A. J. Amaratunga, W. I. Milne, and P. Legagneux, *Nano Lett.* **4**(9), 1575 (2004).